ORIGINAL ARTICLE

Unveiling Nb–Ta mineralization processes: Insight from quartz textural and chemical characteristics in the Songshugang deposit, Jiangxi Province, South China

Hengsong Zhang[1,2] · Shaohao Zou[1] · Xilian Chen[1] · Deru Xu[1,2] · Zhilin Wang[3] · Yongwen Zhang[4] · Hua Wang[1,2]

Abstract The Songshugang deposit is a large Ta–Nb deposit in South China, with Ta–Nb mineralization associated genetically with the granite and pegmatite. A diversity of quartz from topaz–albite granite, quartz–mica pegmatite, quartz–feldspar pegmatite, and quartz–fluorite pegmatite at Songshugang was studied by CL and LA–ICP–MS in order to constrain enrichment mechanisms of Nb and Ta and to find geochemical indicators of quartz for rare metal deposits. Cathodoluminescence image illuminates a canvas of complexity, the quartz from topaz–albite granite, quartz–mica pegmatite, quartz–feldspar pegmatite, and quartz–fluorite pegmatite, exhibits numerous dark CL streaks, patches, and a series of healed fractures. These textures suggest that the rocks were fractured because of deep crustal pressure, and underwent later hydrothermal metasomatism and quartz filling. The quartz from quartz–fluorite pegmatite present limited patches or fractures but distinct growth bands, indicating that the melt fluid composition during the formation of quartz at this stage varies greatly and is less affected by mechanical fragmentation. The LA–ICP–MS analysis of quartz shows that there is a positive correlation between Al and Li in the quartz from topaz–albite granite, quartz–mica pegmatite, quartz–feldspar pegmatite, to quartz–fluorite pegmatite, indicating that Al mainly enters the quartz lattice through charge compensation substitution mechanism with Li. However, our data deviate from the theoretical Li:Al mass ratio of ~ 1:3.89 in quartz, indicating that there may be competition between H^+ and Li in a water-rich magmatic environment. The quartz from topaz–albite granite is enriched in K and Na elements, and the quartz from quartz–fluorite pegmatite is enriched in fluorite with a low Ca content in quartz, further elucidating that these rocks were subjected to hydrothermal metasomatism. From topaz–albitite granite to quartz–fluorite pegmatite, Al, Li and Ge content and Al/Ti, Ge/Ti, Sb/Ti ratios in quartz gradually increased, but Ti content gradually decreased, reflecting the high evolution of magma, which can enrich rare metal elements. Based on the characteristics of quartz CL textures and trace elements in topaz–albite granite, quartz–mica pegmatite, quartz–feldspar pegmatite, and quartz–fluorite pegmatite, combined with the albitization and K-feldspathization of rocks, it is suggested that the Nb–Ta mineralization in Songshugang may be influenced by the combined action of magmatic crystallization differentiation and fluid metasomatism. By comparing the quartz in the Songshugang pluton with the quartz in the granite type and pegmatite type rare metal deposits recognized in the world, the Songshugang pegmatite share similarities with the LCT-type pegmatite. Combined with previous studies, the Ge/Ti > 0.1 and Ti < 10 ppm, as well as Al, Li, Ge, Sb, K, Na contents and Al/Ti, Sb/Ti ratios in quartz have the potential to be a powerful exploration marker for identifying granite-like pegmatitic Nb–Ta deposits in other places.

✉ Shaohao Zou
shaohaozou@hotmail.com

1 State Key Laboratory of Nuclear Resources and Environment, East China University of Technology, Nanchang 330013, Jiangxi, China

2 School of Earth Sciences, East China University of Technology, Nanchang 330013, Jiangxi, China

3 Key Laboratory of Metallogenic Prediction of Nonferrous Metals and Geological Environment Monitoring, Ministry of Education, School of Geosciences and Info-Physics, Central South University, Changsha 410083, China

4 Jiangxi Mineral Resources Guarantee and Service Center, Nanchang 330025, Jiangxi, China

1 Introduction

Niobium (Nb) and tantalum (Ta) are critical metals in modern society due to their wide use in multiple industries, such as aerospace, superconductivity, civil, and military. With the rapid development of China, the demand for Nb and Ta has been increasing gradually (He et al. 2018; Deng et al. 2019), which calls for a further understanding of the origins, enrichment mechanisms, and mineralization processes of these elements in rare metal deposits (Akoh et al. 2015; Melcher et al. 2015; Goodenough et al. 2018; Siegel et al. 2018). The most important Ta–Nb deposits are associated with granite and pegmatite (Linnen et al. 2014). Although many studies have been conducted on the granite- and pegmatite-related Ta–Nb mineralization, there is still a debate on the genesis of the ore formation: (1) owing to the highly incompatible nature of Nb and Ta and their low partition coefficients between fluid and melt, some researchers point out that the Nb and Ta mineralization are mainly controlled by the highly degree of magma fractionation (Thomas et al. 2005; Breiter et al. 2005; Jarchovský 2006; Nardi et al. 2012); (2) The Nb and Ta mineralization is intricately linked to fluid metasomatism based on the empirical observations that Nb–Ta mineralization correlates closely with hydrothermal alterations such as albitization, greisenization, and fluoritization (Xie et al. 2015, 2016; Zhu et al. 2015); (3) The genesis of Nb–Ta mineralization is both associated with the high differentiation of magma and the pronounced fluid metasomatism based on the systemic studies on mica (Wang et al. 2012; Jiang 2020). Therefore, identifying the magmatic hydrothermal evolution process of Nb–Ta deposits is of great significance for understanding the formation of rare metals and formulating corresponding exploration strategies.

Quartz is one of the most important rock-forming minerals, widely occurring in different types of igneous rocks (Götze 2009). In recent years, with the continuous development of modern analytical techniques such as LA–ICP–MS, Cathodoluminescence (CL), EPMA, and SIMS, quartz has become a mineral of choice for conducting research (Watt et al. 1997; Müller et al. 2003; Ruffini et al. 2002; Van Den Kerkhof et al. 2004; Rusk 2006). A large number of studies have shown that the cathodoluminescent structure and trace elements of quartz can be used to constrain temperature, pressure, and pH in the process of magmatic-hydrothermal evolution (Wark and Watson 2006; Rusk et al. 2008; Breiter and Müller 2009; Thomas et al. 2010; Rottier and Casanova 2021), and can be applied as geochemical indicators

for mineral exploration (Jacamon and Larsen 2009; Larsen et al. 2009; Breiter et al. 2020; Rottier and Casanova 2021).

The Songshugang deposit is in Jiangxi Province, in the Qin-Hang Belt of the South China Block. It is a super-large Nb–Ta polymetallic deposit with reserves of about 4.2 kt Ta, at an average grade of 0.0143% Ta_2O_5, and about 6.3 kt Nb, at an average grade of 0.0212% Nb_2O_5 (prospecting report by Jiangxi Nonferrous Metals Geological Exploration Bureau 2018; Zhu et al. 2018). The mineralization is closely associated with the topaz–albite granite and pegmatite at Songshugang (Huang 1999; Zhu et al. 2015; Zhong and Ji 2017; Che et al. 2019). Although previous researchers have systematically examined the geological features, ore-forming age, and geochemical characteristics of Nb and Ta minerals in its deposit (Huang 1999; Zhu et al. 2015; Che et al. 2019), there is still a lack of research on the magmatic differentiation evolution and hydrothermal alteration processes of the Songshugang deposit, which limits our understanding on the Nb–Ta mineralization. Therefore, in this study, we have conducted systematic texture and chemical analyses of quartz in both topaz–albite granite and pegmatite to reveal the extent of magmatic evolution, the influence of hydrothermal alteration, and the enrichment mechanisms of Nb and Ta in the Songshugang deposit. Furthermore, we compare the trace elements in the quartz from the Songshugang deposit to the quartz from globally recognized granite-type or pegmatite-type rare metal deposits and then find geochemical indicators of quartz for rare metal deposits.

2 Geological background

2.1 Regional geology

The South China Block is constituted by the Cathaysia Block in the southeast and the Yangtze Block in the northwest (Fig. 1a). Within the basement of the South China Block, there is a prevalence of Neoproterozoic metamorphic rocks, accompanied by Nanhua–Silurian mudstone–sandstone sequences, pyroclastic formations, and intermediate-basic volcanic compositions (Li et al. 2021). The sedimentary overlying the basement primarily comprises the Carboniferous to Lower Triassic carbonate rocks and mudstone, along with Upper Triassic to Paleogene continental clastic rocks and volcanic rocks (Li et al. 2021). Structural faults are notably developed within South China Block, with the NE-trending Qinzhou–Hangzhou fault standing as the principal fault (Li et al. 2021; Fig. 1b). The region underwent multiple stages of tectonic–magmatic activities, resulting in extensive emplacement of granitic magma (Wang and Zhou 2005; Fig. 1b). Notably, magmatic occurrences were prevalent during the Caledonian (542–360 Ma), Indosinian (250–200 Ma), and Yanshan periods (200–65 Ma), which

Fig. 1 Geological map of South China (after Zhu et al. 2018, 2019; Wang et al. 2023)
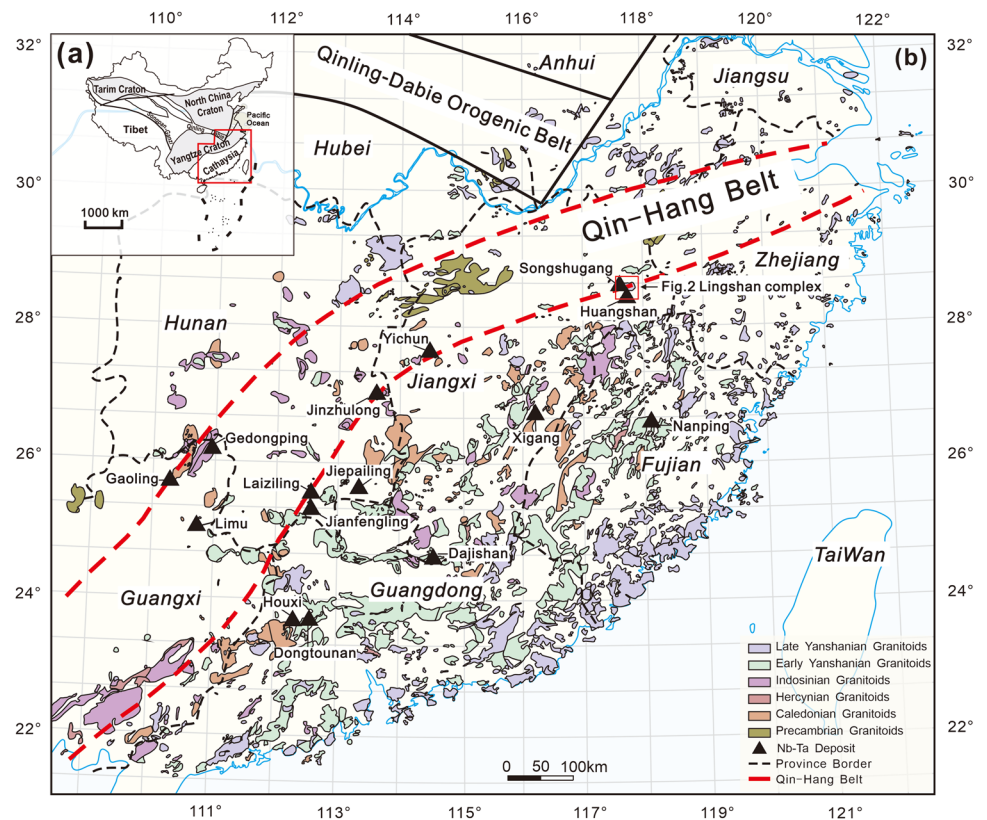
are closely associated with polymetallic mineralization (Sun 2006). Within these periods, the Yanshanian granites are most widespread, constituting approximately 65% of the total granite found in the South China Block, and are economically significant (Hua et al. 2005; Mao et al. 2010). Previous studies revealed that three major Mesozoic mineralizations are genetically related to the Yanshanian granites: (1) Initial mineralization (180–170 Ma) involving Cu, Pb, Zn, and Au. (2) Subsequent mineralization (150–139 Ma) associated with rare metals like W, Sn, Nb, and Ta. (3) Late mineralization phase (125–98 Ma) encompassing Sn, U, Au, Cu, Pb, Zn, Ag, and other metals (Hua et al. 2005).

The Lingshan complex, located in northeastern Jiangxi Province, China, represents a significant Late Mesozoic granite intrusion within the Qin-Hang belt of the center South China Block (Fig. 1b; Zhou et al. 2006). This ring-shaped pluton (Fig. 2) covers an area of approximately 200 km² and intrudes Neoproterozoic to Cretaceous sedimentary strata which consists primarily of sandstone, shale, slate, and mudstone. The area exhibits complex structural features resulting from multiple tectonic events, with the dominant NE-trending Geyuan–Linjianghu syncline and NE- and NNE-trending faults forming a circular pattern around the complex. The occurrence of the Lingshan complex and the distribution of later granite porphyry were influenced by the structures. Based on the field relationships and petrography, the Lingshan complex consists of coarse-grained biotite

hornblende granite (central facies), medium-coarse-grained biotite granite (transitional facies), and medium–fine-grained biotite granite (marginal facies) (Huang 2003). The ages of these different phases range from 134 to 129 Ma (Xiang et al. 2017; Che et al. 2019; Wang et al. 2023). In the northwest and southwest parts of the Lingshan complex, rare polymetallic deposits such as Songshugang Nb–Ta–W–Sn and Huangshan Nb–Ta, along with adjacent mineralized points, have been discovered (Fig. 2; Wang et al. 1982; Xie et al. 2015; Zhu et al. 2015).

2.2 Deposit geology

The Songshugang Nb–Ta–W–Sn deposit, located 3 km northwest of the Lingshan complex, forms an integral part of the concealed Lingshan complex (Fig. 2). The mining area is situated in the northwest wing of the Geyuan-Linjianghu composite syncline (Fig. 2). The prevailing fault trends in the region predominantly follow a NE direction, with minor faults exhibiting NNE and NW orientations (Fig. 3a). Within the mining area, a diverse range of strata is exposed, ranging from the Neoproterozoic Xiuning Formation, Nantuo Formation, Lantian Formation (Fig. 3a; Zhong and Ji 2017). The prominent lithologies encountered in this deposit include phyllite, slate, tuff, and quartz sandstone. In the mine area, only granitic porphyry outcrops at the surface, while the Songshugang pluton itself remains concealed

Fig. 2 Geological map of Lingshan complex (after Zhu et al. 2015)
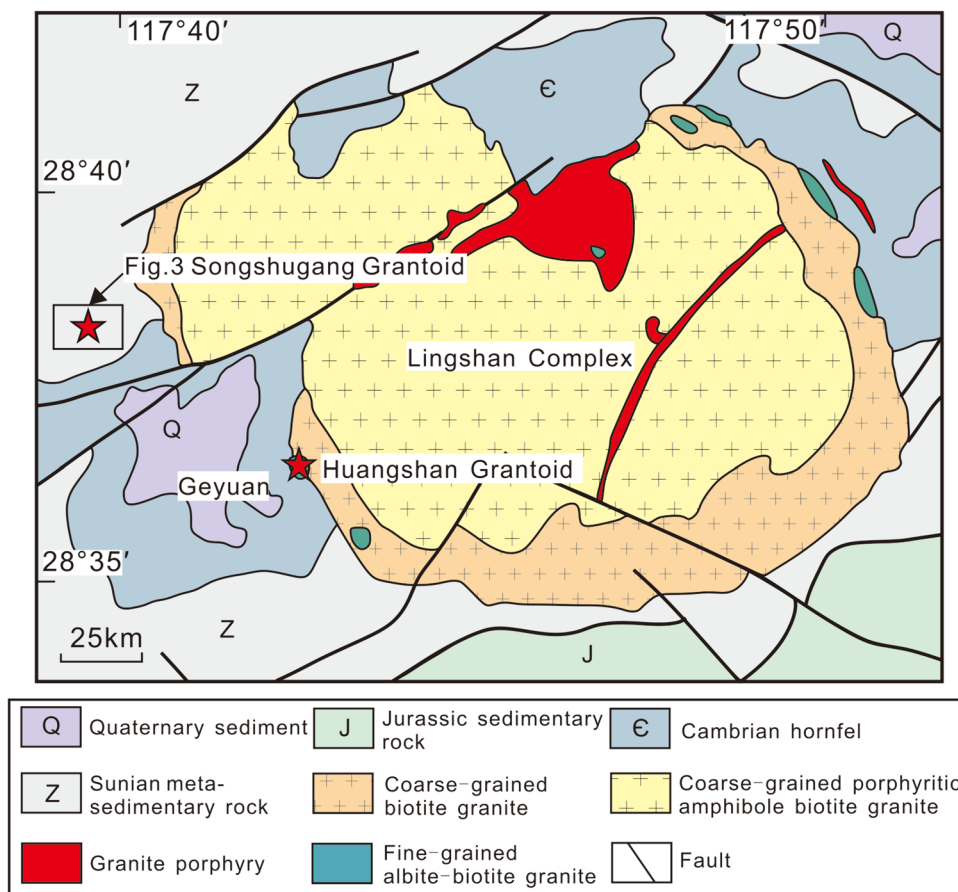
approximately 200 m below ground (Fig. 3b). This concealed intrusion takes the form of an asymmetric bell, characterized by a steep western margin and a gentler eastern slope (Fig. 3b). Previous investigations have classified the rock types within the Songshugang pluton into distinct zones progressing outward from the core: topaz–albite granite, greisen, topaz K-feldspar granite, pegmatite, and late-stage granitic porphyry (Huang 1999; Zhong and Ji 2017; Che et al. 2019; Zhu et al. 2015; Fig. 3b). A remarkable zonal pattern is observed within the pegmatite itself. Quartz–mica pegmatite predominates near the core of the Songshugang intrusion, gradually transitioning to quartz–feldspar pegmatite in the intermediate zone. Further outward, the pegmatite primarily consists of quartz–fluorite pegmatite.

Metallic mineralization in the region exhibits distinct zonation, characterized by two primary types of ore veins. The first type consists of Nb–Ta-dominant veins primarily found within the topaz–albite granite zone. These veins are also observed in the pegmatite, greisen, and topaz K-feldspar granite zones. The second type comprises W-Sn-dominant veins, primarily quartz veins that cut across the Neoproterozoic metamorphic sedimentary rocks. Within the mining area, a diverse range of alteration minerals can be found. These include Zinnwaldite, sericite, K-feldspar, albite, topaz,

fluorite, tremolite, epidote, and chlorite. It is worth noting that Nb–Ta mineralization predominantly occurs within the zone characterized by albitization, K-feldspathization, greisenization, and topazization (Huang 1999; Zhu et al. 2015).

3 Sampling and analytical methods

3.1 Sampling

To gain a deeper understanding of the mineralization process of Nb and Ta at the Songshugang deposit, we conducted a comprehensive study on the quartz from topaz–albite granite and the different types of pegmatite, including quartz–mica pegmatite, quartz–feldspar pegmatite, and quartz–fluorite pegmatite. Based on petrology observations, quartz grains without visible cracks and mineral/fluid inclusions were selected for SEM-CL and LA–ICP–MS analyses.

3.2 Analytical methods

The quartz CL imaging was carried out at the Uranium Polymetallic Center of the State Key Laboratory of Nuclear Resources and Environment at East China University of
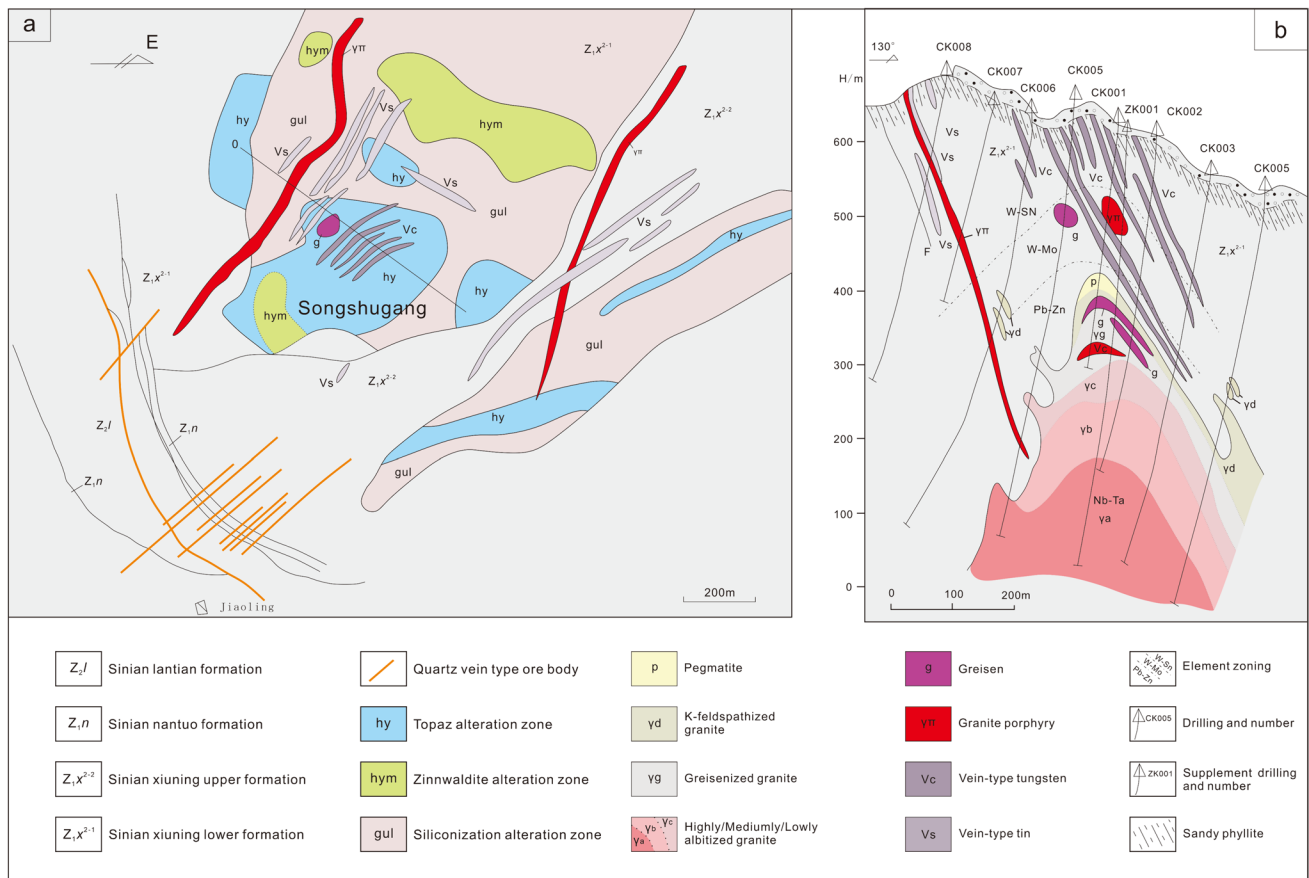
Fig. 3 Geological map of Songshugang mining area (**a**) and profile of exploration Line 0 (**b**) (Liu 2023)

Technology. To prepare the thin sections for analysis, the surface was coated with carbon using an automated carbon coater. Images were then captured using a Zeiss Gemini Sigma 300 VP scanning electron microscope (SEM) equipped with a backscattered electron detector (BSE) and a cathodoluminescence detector. During the imaging process, the SEM operated with an acceleration voltage ranging from 10 to 25 kV, a beam current of 10 nA, and a scanning time of 120 s. Both backscattered images and CL images were captured to reveal the textural characteristics of the different quartz samples.

Trace element analysis in quartz was performed at the Uranium Polymetallic Center of the State Key Laboratory of Nuclear Resources and Environment at East China University of Technology. A PerkinElmer NexION 1000 ICP–MS coupled with an NWR 256femo laser ablation system was employed. The analyses utilized a 40 µm diameter spot with a repetition rate of 8 Hz and a laser fluence of 4 J/cm^2. Each ablation lasted for 45 s, preceded by a 30-s warm-up, and followed by a 30-s washout period. NIST610 served as the primary reference material, while NIST612 and NIST614 were used for data quality assessment. Every 10 samples were interspersed with 2 measurements of NIST610, 2

measurements of NIST612, and 1 measurement of NIST614. The experiment analyzed the following elements: ^{7}Li, ^{11}B, ^{23}Na, ^{25}Mg, ^{27}Al, ^{31}P, ^{39}K, ^{44}Ca, ^{47}Ti, ^{55}Mn, ^{69}Ga, ^{72}Ge, ^{75}As, ^{85}Rb, ^{88}Sr, ^{93}Nb, ^{121}Sb, ^{133}Cs, ^{137}Ba, ^{139}La, ^{172}Yb, ^{181}Ta, ^{182}W, ^{208}Pb and ^{238}U. Data reduction was performed using Iolite4 software (Paton et al. 2011). The internal standard was ^{29}Si, and abnormal signals arising from mineral or fluid inclusions were excluded during data processing.

4 Result

4.1 Petrography

Based on the field cross-cutting relationship and petrographic observations, the formation sequence of the sampled rocks is the topaz–albite granite, followed by quartz–mica pegmatite, quartz–feldspar pegmatite, and quartz–fluorite pegmatite. This established sequence provides invaluable insights into the evolutionary history of these rocks and contributes significantly to our understanding of mineralization processes.

The topaz–albite granite exhibits a porphyritic texture (Fig. 4a, b), with phenocrysts consisting primarily of quartz (10%) and albite (5%). The quartz phenocrysts exhibit euhedral to subhedral granular morphology, ranging in size from 0.5 to 1.3 mm, while the albite phenocrysts display a subhedral tabular texture, ranging in size from 0.8 to 1.5 mm. The groundmass is primarily composed of quartz (40%), feldspar (30%), mica (10%), and topaz (5%). The quartz (Qtz1) in groundmass appears as subhedral grain filling the interstices. The ore mineral is mainly columbite–tantalite. In the CL image, the phenocryst quartz exhibits moderate CL intensity with a uniform brightness and is characterized by numerous dark CL streaks, patches, and healed fractures, without growth zoning (Fig. 4c).

The quartz–mica pegmatite exhibits a pegmatitic texture (Fig. 4d, e), occurring in form as veins cutting through the wall rocks. The principal minerals are quartz and mica, where quartz shows a subhedral texture with a grain size of 1–2 cm, and mica exhibits a fan-shaped texture with a grain size of 0.2–1.2 cm. Ore minerals in the quartz–mica pegmatite include columbite–tantalite, wolframite, and sphalerite. In the CL image, the quartz (Qtz2) in quartz–mica pegmatite shows moderate CL intensity with the development of dark CL streaks, patches, and healed fractures, without growth zoning (Fig. 4f).

The quartz–feldspar pegmatite exhibits a pegmatitic texture (Fig. 4g, h) with the main minerals consisting of quartz and feldspar. Quartz displays subhedral textures with grain
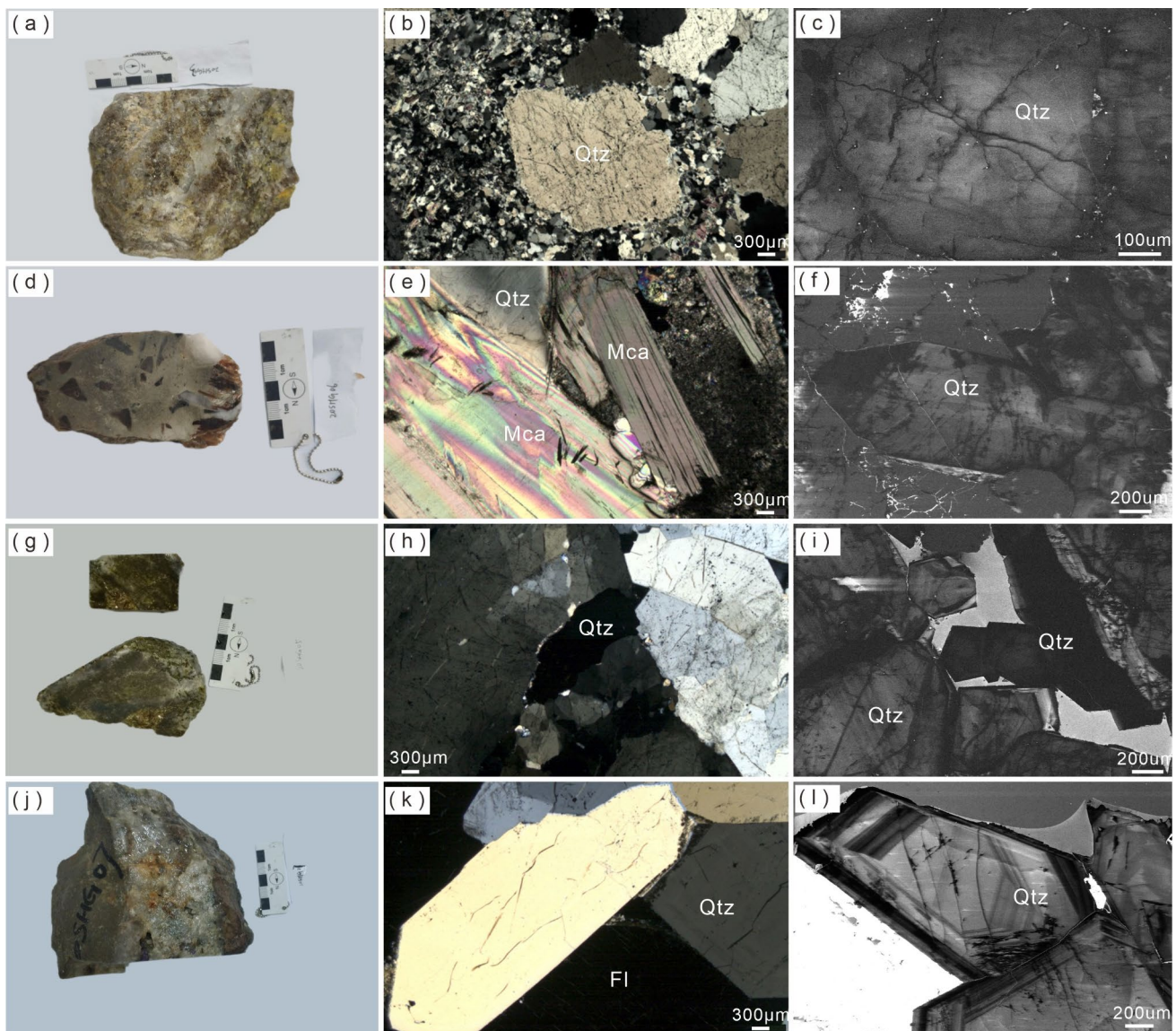

Fig. 4 Photographs of the different rocks in the Songshugang pluton, **a–c** topaz–albite granite; **d–f** quartz–mica pegmatite; **g–i** quartz–feldspar pegmatite; **j–l** quartz–fluorite pegmatite; Qtz-quartz; Mca-mica; Fl- fluorite

sizes ranging from 0.5 to 1.5 cm, while feldspar exhibits subhedral tabular textures with grain sizes ranging from 0.7 to 2 cm. The ore minerals in the quartz–feldspar pegmatite comprise columbite–tantalite and sphalerite. In the CL image, the quartz (Qtz3) in the quartz–feldspar pegmatite shows low CL intensity with the development of dark CL streaks, patches, and healed fractures, without growth zoning (Fig. 4i).

The quartz–fluorite pegmatite exhibits a pegmatitic texture (Fig. 4j, k), characterized by quartz and fluorite as the main minerals. Quartz displays euhedral to subhedral structures with grain sizes ranging from 0.2 to 0.7 cm, and fluorite aggregates fill the voids. The ore minerals within the quartz–fluorite pegmatite are primarily columbite–tantalite, pyrite, and jacobsite, with small amounts of xenotime and galena. In the CL image, the quartz (Qtz4) shows high CL

intensity with limited dark CL patches or healed fractures but distinct growth zoning (Fig. 4l).

4.2 Trace element compositions of quartz

Table 1, Appendix A and Fig. 5 provide the results of the trace element analysis results for the different types of quartz. Notably, Al and Ca significantly exhibit higher levels compared to other elements, while Li, Na, K, Ti, Ge, Sb, and other elements have relatively lower contents. The variation trends of trace elements differ among the various quartz types. Specifically, Li and Al elements display largely consistent trends across all types, whereas the contents of Ti, Na, and K elements demonstrate a gradual decrease. The contents of Ge and Sb exhibit a bimodal pattern, while Ca

Table 1 Trace element compositions (ppm) and ratios in quartz of Songshugang granite and pegmatite

	Li	Na	Al	K	Ca	Ti	Ge	Sb	Al/Li	Al/Na	Al/K	Al/Ge	Al/Ti	Ge/Ti	Sb/Ti	Ge+Sb/Ti
Qtz1																
MAX	18.8	298	187	218	237	32.3	2.07	0.30	32.4	55.5	10.3	802	14.4	0.12	0.02	0.13
MIN	4.64	2.09	107	17.1	128	11.6	0.17	0.01	7.39	0.48	0.54	57.7	4.56	0.01	–	0.02
Mean	13.0	59.4	143	59.5	178	19.3	0.90	0.18	12.3	13.1	3.65	335	8.32	0.05	0.01	0.06
Qtz2																
MAX	34.1	81.8	436	38.9	423	18.6	5.01	3.67	644	306	3699	631	76.1	1.21	0.91	1.65
MIN	0.11	0.34	27.6	0.05	210	1.66	0.17	0.06	5.49	1.16	4.89	9.33	3.94	0.03	0.01	0.08
Mean	14.6	17.0	154	4.05	296	8.18	2.03	0.62	26.5	48.3	378	99.2	21.0	0.30	0.1	0.43
Qtz3																
MAX	84.5	140	614	6.02	560	8.63	1.64	1.31	21.8	56 .0	243	614	675	2.74	1.39	2.76
MIN	0.93	0.95	3.27	1.29	369	0.31	1.00	0.01	6.16	0.43	2.53	2.07	1.10	0.16	0.01	0.2
Mean	12.1	24.2	103.9	3.21	428	4.30	1.33	0.35	11.0	21.5	53 .6	91.5	84.0	0.60	0.24	0.78
Qtz4																
MAX	336	43.4	2696	17.9	357	2.49	8.36	6.55	18.0	7725	4569	1388	30,396	47.3	48	95.3
MIN	0.38	0.28	13.9	0.24	222	0.03	0.25	0.04	3.78	7.78	21.4	10.4	48.0	0.19	0.07	0.25
Mean	100	15.9	739	2.09	300	0.98	2.89	1.31	7.58	666	623	272	2094	5.94	3.37	9.44

"–"indicates less than 0.01

Fig. 5 Box plot of main trace elements in different types of quartz. The height of the colored bars represents the interquartile range (25%–75%). The horizontal-colored lines within the colored boxes are the median value and the colored squares represent the mean. "Whiskers" of each box extend to the extremum values lying within 2.0 times the interquartile range beyond the edges of the box. The colored circles represent the outliers deviating
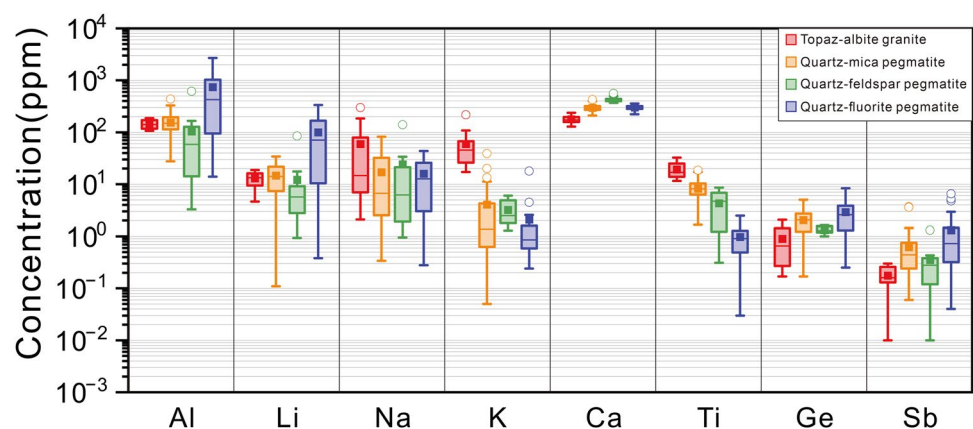
content shows a distinct increase followed by a decrease (Fig. 5).

The analysis reveals a wide variation range in the Al content of quartz, spanning from 3.27 to 2696 ppm. The quartz from topaz–albite granite and quartz–mica pegmatite exhibit relatively stable Al content, averaging 143 and 154 ppm, respectively. In contrast, the quartz from quartz–feldspar pegmatite displays lower Al content (103.9 ppm), while the quartz from quartz–fluorite pegmatite exhibits a significant range (13.9–2696 ppm) and a higher average (739 ppm). Similar to Al, Li content also exhibits a broad range (0.11–336 ppm). The quartz from topaz–albite granite and quartz–mica pegmatite demonstrates relatively stable Li content (13.0 and 14.6 ppm on average, respectively). The quartz from quartz–feldspar pegmatite shows lower average Li content (12.1 ppm), while the quartz from quartz–fluorite pegmatite has a higher average (100 ppm) and wider range (0.38–336 ppm). The Ca contents in all quartz exhibit considerable overlap, ranging from 128 to 560 ppm. The quartz from quartz–feldspar pegmatite shows slightly higher Ca values (369–560 ppm) with an average of 428 ppm. The Ca content gradually increases from the quartz in topaz–albite granite, to quartz–mica pegmatite and quartz–feldspar pegmatite but then experiences a sudden decrease in the quartz from quartz–fluorite pegmatite (average 300 ppm). The Ge content in the different types of quartz remains relatively stable, ranging from 0.17 to 8.36 ppm. In contrast, the Ti content gradually decreases from the quartz in topaz–albite granite, to quartz–mica pegmatite, quartz–feldspar pegmatite, and quartz–fluorite pegmatite (19.3, 8.18, 4.30, and 0.98 ppm on average, respectively). The Na and K content ranges from 0.28 to 298 ppm and 0.05 to 218 ppm, respectively, with the quartz from topaz–albite granite exhibiting higher values compared to another. The average Na content is 59.4 ppm, while the average K content is 59.5 ppm. The Sb content in various quartz types is relatively low, ranging from 0.01 to 6.55 ppm.

Figure 6 presents the ratios of trace elements in different types of quartz, revealing distinct trends. The Al/Li ratio ranges from 7.39 to 32.4 in the quartz from topaz–albite granite, 5.49–644 in the quartz from quartz–mica pegmatite, 6.16–21.8 in the quartz from quartz–feldspar pegmatite, and 3.78–18.0 in the quartz from quartz–fluorite pegmatite. The Al/Ti ratio increases from the quartz in topaz–albite granite (4.56–14.4), to quartz–mica pegmatite (3.94–76.1), quartz–feldspar pegmatite (1.10–675), and quartz–fluorite pegmatite (48.0–30396). The Ge/Ti ratio increases from the quartz in topaz–albite granite (0.01–0.12), to quartz–mica pegmatite (0.03–1.21), quartz–feldspar pegmatite (0.16–2.74), and quartz–fluorite pegmatite (0.19–47.3). The Sb/Ti ratio increases gradually, with averages of 0.01 (the quartz from topaz–albite granite), 0.10 (the quartz from quartz–mica pegmatite), 0.24 (the
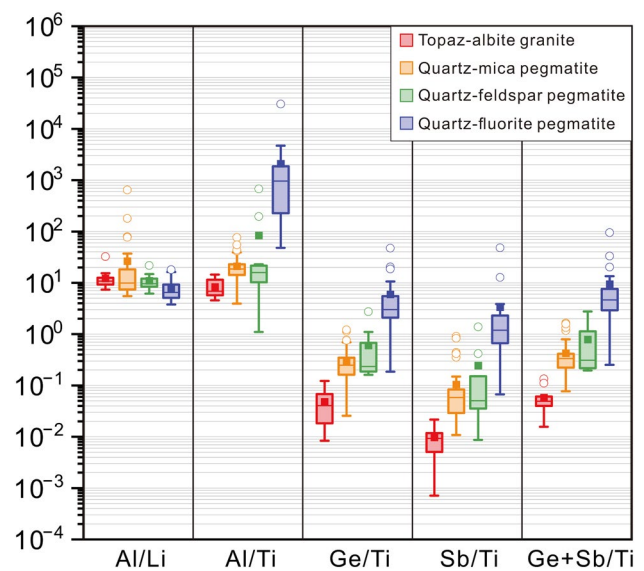

Fig. 6 Box plot of main trace elements ratios in different types of quartz. Box plot statistical parameters are as mentioned in Fig. 5

quartz from quartz–feldspar pegmatite), and 3.37 (the quartz from quartz–fluorite pegmatite). The overall average of (Ge + Sb)/Ti also increases gradually, with averages of 0.06 (the quartz from topaz–albite granite), 0.43 (the quartz from quartz–mica pegmatite), 0.78 (the quartz from quartz–feldspar pegmatite), and 9.44 (the quartz from quartz–fluorite pegmatite).

Figure 7 reveals intriguing relationships between trace elements in quartz. The data from the Songshugang quartz demonstrate a positive correlation between Al and Li, with a majority of points falling below the Li/Al isopleth of 1:3.89 (Fig. 7a). Additionally, a close association exists between Al and Ge, suggesting a positive correlation (Fig. 7b). In contrast, Ti and Ge exhibit a clear negative correlation, with Ti content gradually decreasing and Ge content increasing from the quartz in topaz–albite granite, to quartz–mica pegmatite, quartz–feldspar pegmatite, and quartz–fluorite pegmatite (Fig. 7c). The relationships of Al/Ti with Sb/Ti, Ge/Ti, and (Ge + Sb)/Ti all show strong positive correlations (Fig. 7d–f). These relationships collectively demonstrate an increasing trend in Al, Li, Ge, and Sb content as Ti content decreases, as evidenced by the quartz data transitioning from topaz–albite granite, quartz–mica pegmatite, quartz–feldspar pegmatite, to quartz–fluorite pegmatite. However, the data from the Songshugang quartz demonstrate no obvious correlation between Al, K, and Li (Fig. 7g–h).

While quartz in topaz–albite granite, mica-pegmatite, and feldspar–pegmatite lacked discernible CL response, the quartz from quartz–fluorite pegmatite displays distinct growth banding (oscillatory zone). To explore the potential relationship between CL intensity and trace elements in
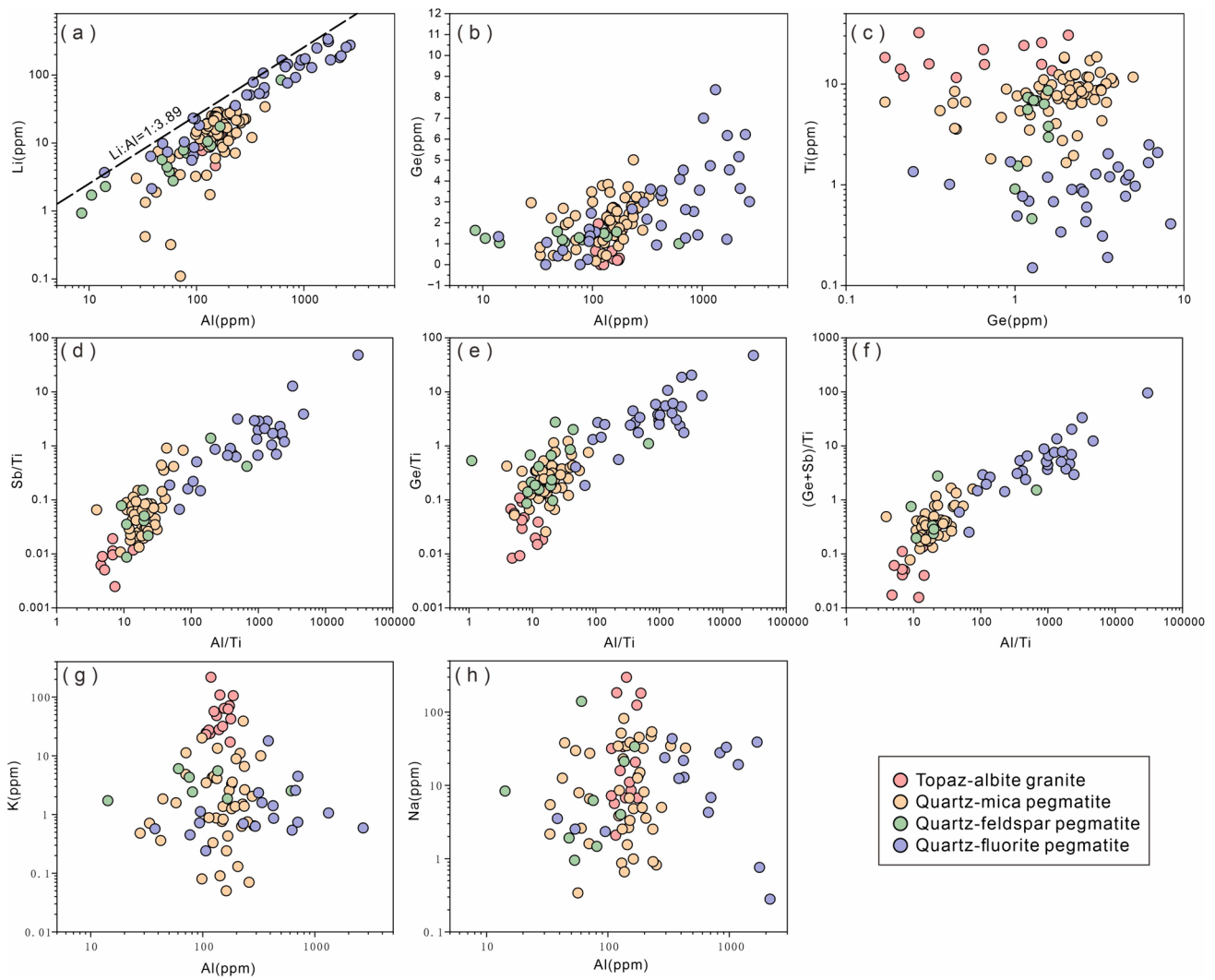
Fig. 7 Correlation diagram of trace element in quartz. **a** Li Vs Al; **b** Ge Vs Al; **c** Ti Vs Al; **d** Sb/Ti Vs Al/Ti; **e** Ge/Ti Vs Al/Ti; **f** (Ge + Sb)/Ti Vs Al/Ti; **g** K Vs Al; **h** Na Vs Al

quartz, we specifically selected samples from this banded variety, as shown in Fig. 8. Notably, brighter regions in the quartz consistently correspond to significantly higher Al and Li concentrations compared to their darker counterparts. In Fig. 8a, point 7 exhibited the highest CL intensity and Al and Li contents, with values reaching 2696 and 275 ppm, respectively. Similar findings were observed in Fig. 8b, with point 4 having the highest CL intensity alongside peak Al and Li concentrations of 1695 and 310 ppm, respectively. In Fig. 8c, point 2 displayed the strongest CL intensity and highest Al and Li content, reaching 1679 and 336 ppm, respectively. Furthermore, the relatively brighter points 1 and 2 consistently had higher Al and Li contents compared to the darker points 3, 4, 5, 6, and 7. Finally, in Fig. 8d, point 5 exhibited the highest CL intensity and peak Al and Li contents of 614 and 84.5 ppm, respectively. The remaining bands in this figure had Al and Li contents below 8 ppm, with the relatively

brighter parts (points 6–10) showing higher concentrations compared to the darker regions (points 1–4).

5 Discussion

5.1 Petrogenesis implications of CL texture in quartz

Diverse defects within mineral crystals, both intrinsic and arising from impurities, alter local optical properties, giving rise to distinct CL characteristics. Specific types and distributions of these defects impact the intensity and pattern of CL in minerals (Stevens-Kalceff 2009; Leeman et al. 2012). Consequently, CL textural patterns, revealed by the SEM-CL technique, serve as sensitive indicators of changes in external conditions experienced by the mineral (e.g., Kanaori

Fig. 8 Relationship between quartz CL intensity and trace element content (ppm); **a–c** quartz–fluorite pegmatite; **d** quartz–feldspar pegmatite; the missing data in the Ti content is due to being below the detection line
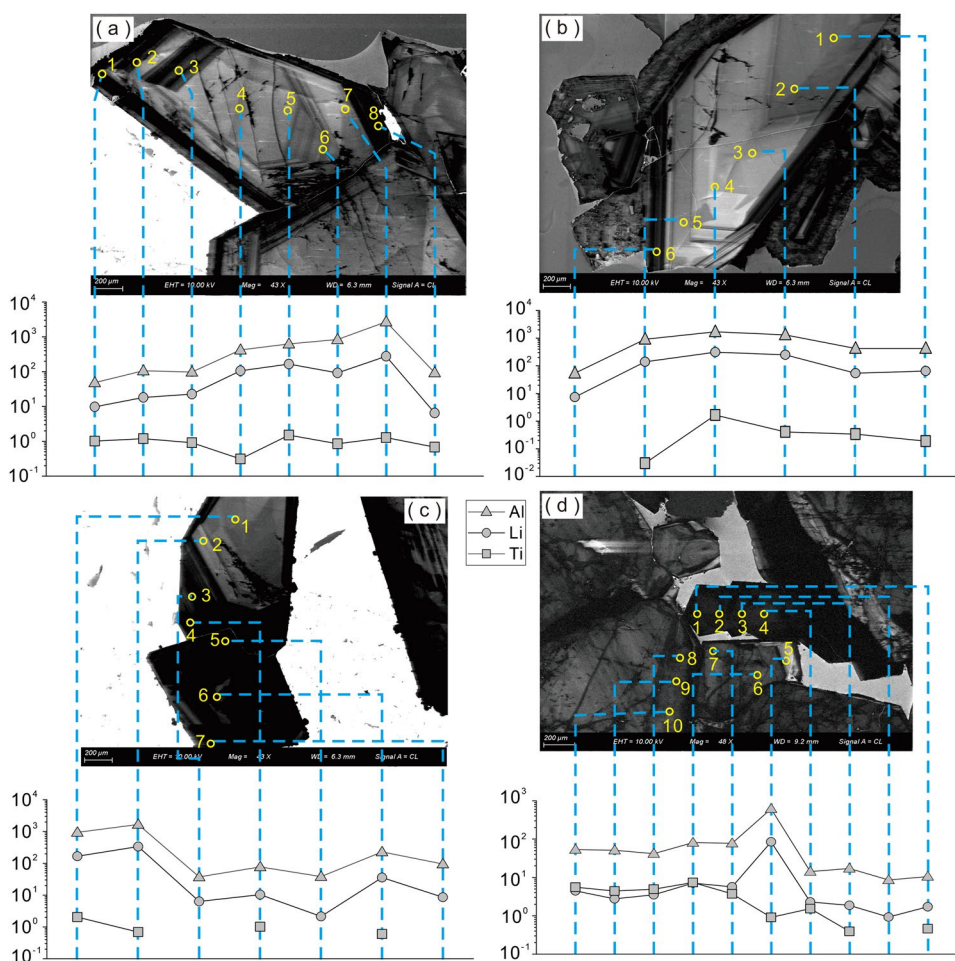
1986; Seyedolali et al. 1997; Bernet and Bassett 2005; Müller et al. 2005; Larsen et al. 2009; Rusk 2012).

Under SEM-CL, quartz reveals microstructures that are not observed under optical microscopes, such as dark CL streaks and patches, healed fractures, and growth zoning (Seyedolali et al. 1997; Bernet and Bassett 2005; Rusk et al. 2008). Our study examined CL images of the quartz from the Songshugang pluton and revealed diverse features. The quartz from topaz–albite granite, quartz–mica pegmatite, and quartz–feldspar pegmatite, exhibits numerous dark CL streaks and patches, and a series of healed fractures under CL, devoid of obvious growth zoning (Fig. 4b, e, h), whereas, the quartz from quartz–fluorite pegmatite present limited dark CL patches or healed fractures but distinct growth bands (Fig. 4k). The dark CL streaks, patches, and healed fractures in quartz is closely linked to changes in deep crustal pressure that leads to mechanical fragmentation of quartz, then followed by dissolution during hydrothermal alteration. The fragments and dissolved primary quartz are subsequently filled by later, non-luminescent quartz, and quartz–fluorite pegmatite is less affected by mechanical fragmentation (Seyedolali et al. 1997; Schieber et al. 2002).

In contrast, the quartz from quartz–fluorite pegmatite exhibits distinct growth CL zoning with clear core-rim differences (Fig. 8). On the one hand, this zoning likely reflects periodic variations in magma-fluid composition during crystal growth. On the other hand, potentially results from multiple evolutionary stages involving dissolution, precipitation, and re-dissolution (Landtwing and Pettke 2005; Larsen et al. 2009; Müller et al. 2010; Hong et al. 2020). These variations are likely influenced by the distribution of trace element content within the quartz, leading to alternating bright and dark variations in the CL zones. Significantly different Al, Li, Ge, and Sb concentrations observed in quartz from quartz–fluorite pegmatite (Table 1, Fig. 5) corroborate the potential influence of evolving magma-hydrothermal components during its growth. Imbalances in trace element incorporation into the quartz lattice likely contributed to the formation of those bands (Götze et al. 2001; Rusk et al. 2008; Stevens-Kalceff 2009; Lehmann et al. 2011). Notably, the broader core bands with higher luminescence intensity compared to the narrower, less luminescent rim bands suggest a decrease in element incorporation as the quartz developed. This may be attributed to the gradual depletion of elements like Al

and Li from the residual magma alongside rapid changes in temperature and pressure.

In addition, our study confirms a strong correlation between the intensity of CL and the presence of Al and Li in the quartz, while no such link is observed with Ti (Watt et al. 1997; Rusk et al. 2008; Müller et al. 2012). Brighter quartz areas or bands consistently contain significantly higher Al and Li content compared to darker areas (Fig. 8), suggesting these elements play a key role in CL intensity for Songshugang quartz. Interestingly, the CL intensity of quartz from topaz albitite granite and quartz–mica pegmatite is consistent (Fig. 4c, f), but the CL intensity of quartz from quartz–feldspar pegmatite decreases (Fig. 4i), and then the CL intensity of quartz from quartz–fluorite pegmatite increases and is the highest (Fig. 4l), which correlates the trend of Al and Li contents (Fig. 5). The weakening of quartz CL intensity of quartz–feldspar pegmatite may be caused by the competition between feldspar and quartz for Al, which reduces the amount of Al entering the quartz lattice and affects the CL intensity. However, Al^{3+}, with compensated Li^+, replaces Si^{4+}, and the corresponding Li is also reduced (Fig. 7a).

Overall, the study of CL characteristics of quartz highlights the impact of late-stage hydrothermal alteration on the Songshugang pluton formation, evident through the CL characteristics of its quartz. Furthermore, these characteristics offer valuable insights into the evolution and genesis processes of rocks, as well as changes in their surrounding environment.

5.2 Incorporation implications of trace elements in quartz

Previous studies have suggested that trace elements in quartz are mainly affected by mineral/fluid inclusions or via isomorphic substitution of Si^{4+} in the lattice (Czamanske et al. 1963; Götze et al. 2004; Rottier and Casanova 2021). By focusing on smooth segments in LA–ICP–MS depth profiles, we exclude anomalous signals from inclusions, ensuring our data reflect elements solely incorporated via lattice substitution. Understanding the mechanisms governing this substitution is crucial for unraveling the formation process of quartz (Götze et al. 2004; Larsen et al. 2004; Jacamon and Larsen 2009).

In the Songshugang deposit, our data reveals that isomorphic substitution primarily involves tetravalent ions like Ti^{4+} and Ge^{4+} replacing Si^{4+}. Additionally, a strong positive correlation between Al and Li in Fig. 7a indicates coupled substitution, where Al^{3+} replaces Si^{4+} and balances charges by Li^+ ($Al^{3+} + Li^+ \rightarrow Si^{4+}$). However, our data deviate from the theoretical Li:Al mass ratio of ~ 1:3.89 in quartz (Müller and Koch-Müller 2009; Müller et al. 2021). Since K and Na are also common ions of charge compensation Al,

they have no obvious correlation with Al (Fig. 7g, h), so the competitive relationship with Li is excluded. Intriguingly, literature suggests H^+ can substitute for Li^+ in water-rich environments to balance Al^{3+} (Breiter et al. 2020). Our deviation from the expected Li:Al ratio, along with findings from the literature, strongly suggest that H^+ may be the primary substitute for Li^+, providing compelling evidence for a water-rich magmatic environment during the formation Songshugang deposit.

The changes in the content of Na, K, and Ca elements in Songshugang quartz may reflect the influence of hydrothermal alteration. Figure 5 reveals significantly higher Na and K contents in the quartz from topaz–albite granite compared to granitic pegmatite. This, coupled with the observed abundance of K-feldspar and albite in these rocks, suggests that variations of Na and K content in quartz may reflect the different proportions of K-feldspar and albite in host rock. Calcium contents of quartz exhibit a different variation trend, initially increasing and then decreasing from topaz–albite granite, quartz–mica pegmatite, quartz–feldspar pegmatite, to quartz–fluorite pegmatite (Fig. 5). The initial increase in Ca is probably related to the enrichment of Ca during magmatic differentiation. However, during the late stages of magmatic evolution, Ca ions are likely combined with F ions in the magma-hydrothermal fluid to form fluorite, leading to a decrease in Ca content. This suggests the persistence of significant volatile components within the residual magma-hydrothermal system even during late magmatic evolution.

Previous studies have established a strong link between Al, Ti, and Ge contents in quartz to the degree of magmatic differentiation, specifically, as magma evolves, Al and Ge in the quartz crystallized will increase, whereas, Ti in the quartz will decrease (Schrön et al. 1988; Larsen et al. 2004; Götze et al. 2004; Rottier and Casanova 2021). At Songshugang deposit, the Al content increases in the quartz from topaz–albite granite, quartz–mica pegmatite, quartz–feldspar pegmatite, to quartz–fluorite pegmatite, reaching a peak in quartz–fluorite pegmatite, reflecting Al enrichment in late-stage, volatile-rich magmas (Müller et al. 2000). This implies the Songshugang residual magma was highly evolved and volatile-rich before final crystallization. Similar to the variations of Al, the Ge contents increase in the quartz from topaz–albite granite, quartz–mica pegmatite, quartz–feldspar pegmatite, to quartz–fluorite pegmatite, further supporting the magmas undergo high magmatic fractionation. In contrast, Ti contents in quartz decrease from topaz–albite granite, quartz–mica pegmatite, quartz–feldspar pegmatite, to quartz–fluorite pegmatite (Fig. 5). Compared with other elements, Ti prefers to be incorporated into quartz lattice incorporation, however, it is strongly temperature-dependent (Wark and Watson 2006; Rusk et al. 2008; Thomas et al. 2010). The decreasing trend of Ti in the quartz from topaz–albite granite, quartz–mica pegmatite, quartz–feldspar

pegmatite, to quartz–fluorite pegmatite (Fig. 5) indicates a gradual decreasing crystallization temperature of quartz.

Al/Ti and Ge/Ti in quartz have been established as reliable indicators of magma differentiation, comparable to widely used whole-rock ratios like K/Rb, Rb/Sr, and Zr/Hf (Larsen et al. 2004; Jacamon and Larsen 2009; Rottier and Casanova 2021). Our data reveal systematic variations in these ratios (Fig. 6), both Al/Ti and Ge/Ti in quartz progressively increasing as magmas evolve. This confirms their effectiveness as differentiation indicators for the Songshugang pluton. Supporting this notion, (Rottier and Casanova 2021) highlighted the effectiveness of quartz Al/Ti, Sb/Ti, Ge/Ti, and (Sb + Ge)/Ti ratios in reflecting continuous magma evolution in porphyry systems. All quartz trace element ratios at Songshugang show a distinct increasing trend from topaz–albite granite, quartz–mica pegmatite, quartz–feldspar pegmatite, to quartz–fluorite pegmatite, and each exhibits a strong continuous positive correlation with the Al/Ti ratios (Figs. 6 and 7d–f). This further corroborates the progressive differentiation from topaz–albite granite, quartz–mica pegmatite, quartz–feldspar pegmatite, to quartz–fluorite pegmatite, providing robust evidence for magmatic evolution within the Songshugang pluton.

In summary, the trace elements and their ratios in the quartz from the Songshugang deposit provide valuable insights into its formation. The substitution of Al^{3+} for Si^{4+}, along with the potential involvement of Li^+ and H^+ for charge compensation, suggests a water-rich magmatic environment. Variations in Na, K, and Ca content indicate fluid metasomatism processes. The Al, Ti, and Ge contents, as well as their element ratios like Al/Ti, serve as powerful indicators of differentiation within the Songshugang pluton.

5.3 Genesis of Songshugang deposit

The genesis of Nb–Ta deposits has been a long-standing debate, with competing hypotheses centered on magmatic differentiation and hydrothermal alteration (Van Lichtervelde et al. 2018; Ballouard et al. 2020). The magmatic perspective hinges on the highly incompatible nature of Nb and Ta, leading to their enrichment in residual melts during differentiation. Their extremely low fluid/melt partition coefficients ($D_{Nb}^{fluid/melt}$=0.005-0.08; $D_{Ta}^{fluid/melt}$=0.002-0.08) further substantiate this, emphasizing their preferential concentration in melts over fluids (Linnen 1998; Linnen and Keppler 1997; Zajacz et al. 2008; Zaraisky et al. 2010). Conversely, the hydrothermal perspective highlights the frequent association of Nb–Ta minerals with alteration signatures like albitization and potassic alteration in surrounding rocks (Li et al. 2015; Xiang et al. 2017; Wu et al. 2018), with zones of intense alteration often hosting the highest Nb–Ta concentrations (Wang et al. 2012; Jiang 2020; Zhao et al. 2022).

Our study of the Songshugang deposit sheds light on this longstanding debate, revealing the intricate interplay between both processes. Notably, trace element trends in quartz point towards a highly evolved magmatic system. Increasing Al and Ge content alongside decreasing Ti content indicate progressive differentiation under decreasing temperatures. Furthermore, systematic variations in Al/Ti, Ge/Ti, Sb/Ti, and (Sb + Ge)/Ti ratios, all exhibiting positive correlations with the Al/Ti ratio, further corroborate this trend, mirroring established indicators of differentiation from topaz–albite granite to quartz–feldspar pegmatite.

Beyond magmatic differentiation, our study also underscores the influence of hydrothermal processes. While geochemical evidence alone cannot definitively pin down specific fluid compositions, the observed alteration signatures, combined with the established preference of Nb and Ta for melt enrichment, suggest that fluids likely played a secondary role in redistributing and concentrating these elements within the deposit. Importantly, this highlights the complex interplay between both processes, rather than their mutually exclusive nature, in shaping the final distribution and abundance of Nb and Ta within the Songshugang deposit.

The formation of the Songshugang deposit unfolded as a dynamic interplay of magma differentiation and hydrothermal transformation, ultimately dictating the fate of precious Nb and Ta. In the early stages, intense differentiation sculpted the melt, favoring the enrichment of incompatible elements like Nb and Ta. This enrichment was mirrored in the quartz trace elements, showcasing a gradual increase in Al and Ge alongside a decrease in Ti from topaz–albite granite, quartz–mica pegmatite, quartz–feldspar pegmatite, to quartz–fluorite pegmatite. As differentiation deepened, volatile elements and fluids gradually gained prominence, brewing a late-stage magmatic hydrothermal system brimming with water, mineralizers, and rare metal treasures. These potent fluids ventured beyond the confines of the magma, embarking on a journey of metasomatism within the surrounding rocks. Their touch ignited transformative processes, inducing a kaleidoscope of alterations like albitization, K-feldspathization, and even greisenization. The topaz–albite granite, bearing the brunt of this interaction, displayed the most vivid tapestry of alterations, highlighting a potent exchange between melt and rock.

Intriguingly, the quartz trace elements whisper tales of a water-rich environment. Deviations from the theoretical Li:Al ratio point towards the participation of H^+ in compensating for Al^{3+} during quartz lattice formation. This aqueous setting fostered the formation of complexes between Nb and Ta with alkali metal ions like K^+ and Na^+, further enhancing their mobility and solubility. The dance reached its climax as physical and chemical conditions shifted. Decreasing temperature and pressure, alongside strengthening alkali metasomatism, destabilized the metal complexes. This instability

triggered their graceful transformation, precipitating Nb and Ta minerals within the granites and pegmatites, adorning them with shimmering treasures. Notably, fluorine played a captivating role in this final act. Its presence, evidenced by topaz and fluorite minerals alongside a decrease in Ca in quartz trace elements, suggests an F-rich magmatic-hydrothermal system. This volatile maestro not only influenced mineral crystallization times but also facilitated the further enrichment of Nb and Ta through complex formation.

Therefore, the Songshugang deposit stands as a testament to the intricate synergy between magmatic differentiation and hydrothermal alteration. It is a story of enrichment, transformation, and precipitation, where the stage is set by intense differentiation, the characters introduced through potent fluids, and the final act orchestrated by shifting conditions and the subtle influence of fluorine. This story not only unveils the secrets of the Songshugang deposit but also illuminates the crucial interplay between these processes in shaping the fate of rare metals across the globe.

5.4 Economic implications of quartz

Minerals, silent witnesses to Earth's history, offer a unique record of environmental changes caused by geological processes like magmatic activity and hydrothermal alteration. Their chemical composition and texture, particularly the trace elements within specific minerals like quartz, provide

invaluable insights for exploration activities, especially for deposits rich in rare metals (Breiter et al. 2020). Quartz, one of the most common minerals on Earth (Götze et al. 2004), exhibits trace element variations reflecting the physical and chemical conditions of its formation and subsequent stages of magmatic-hydrothermal evolution (Lehmann et al. 2011; Rottier and Casanova 2021). Analyzing these variations in quartz thus becomes a powerful tool for deciphering past geological evolution processes and, crucially, for identifying potential locations of hidden mineral deposits (Monecke et al. 2002; Larsen et al. 2004; Landtwing and Pettke 2005; Rusk et al. 2008; Breiter et al. 2014; Rottier and Casanova 2021).

Compiling data from existing studies (Larsen et al. 2004; Müller et al. 2008; Müller and Koch-Müller 2009; Beurlen et al. 2011; Breiter et al. 2014, 2020), this study analyzes quartz trace elements from three rare metal-bearing lithologies: S-type granite, LCT-type pegmatite, and NYF-type pegmatite. Our analysis reveals distinct, fingerprint-like signatures within the Songshugang deposit.

The topaz–albite granite at Songshugang, characterized by quartz with relatively high Ti and low Ge content, overlaps with S-type granites and LCT-type pegmatites known for rare metal mineralization (Fig. 9a). Conversely, pegmatites at Songshugang exhibit low Ti and high Al and Ge in their quartz, aligning with LCT-type pegmatites and indicating highly differentiated magmas conducive to rare

Fig. 9 Ternary and binary diagrams of quartz from Songshugang granites and pegmatites, comparing with rare-metal S-type granites, LCT (Li–Cs–Ta) pegmatites, and NYF (Nb–Y–F) pegmatites (Appendix B; Larsen et al. 2004; Müller et al. 2008; Breiter and Müller 2009; Beurlen et al. 2011; Breiter et al. 2014, 2020). **a** Ti-Ge*10-Al/10 ternary diagram of quartz, topaz–albite granite mostly overlaps with rare metal S-type granite, and pegmatite data overlaps with LCT type pegmatite; **b** Ge/Ti Vs Al/Ti binary diagrams; **c** Ge/Ti Vs Ti diagram with yellow area highlighting respective Ge/Ti > 0.1 and Ti < 10 ppm for the threshold that indicates potential typical high evolution magma zone
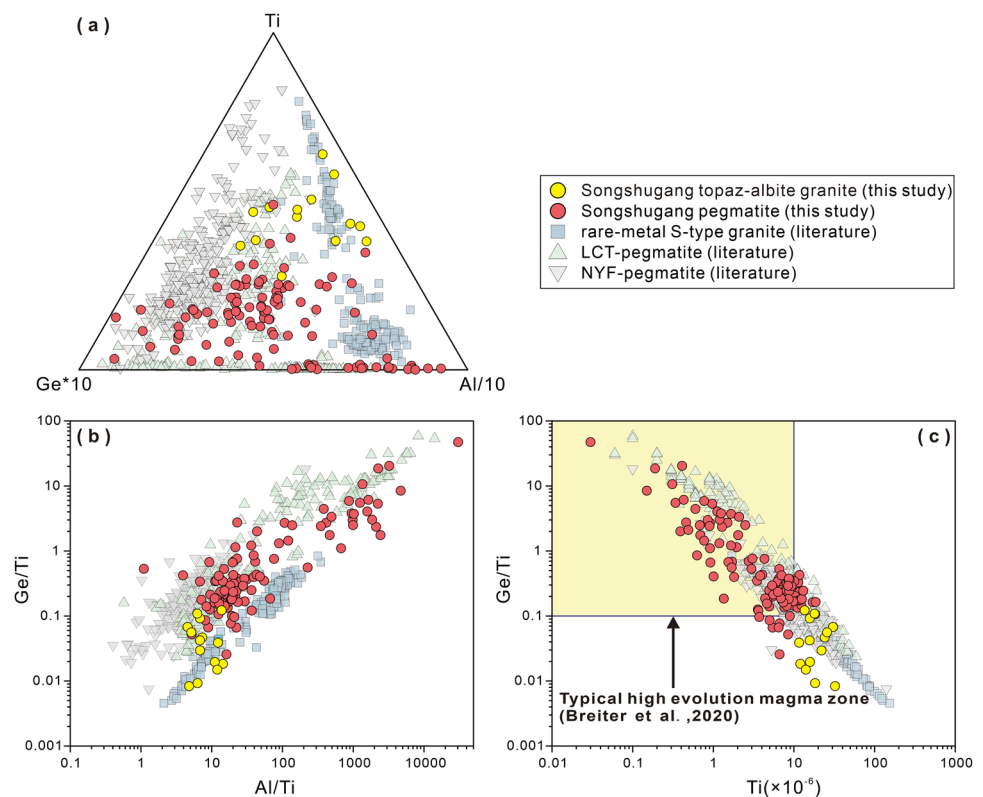
metal enrichment (Fig. 9a). This differentiation trend is further corroborated by Al/Ti and Ge/Ti ratios in quartz, with NYF-type pegmatites displaying the highest Ge/Ti and lowest Al/Ti, while S-type granites exhibit the opposite (Fig. 9b). A progressive increase in Al/Ti and Ge/Ti ratios from topaz–albite granite, quartz–mica pegmatite, quartz–feldspar pegmatite, to quartz–fluorite pegmatite (Fig. 6) provides further support for this differentiation trend within the Songshugang deposit.

These distinct quartz fingerprints hold significant economic potential. Our study reveals contrasting geochemical signatures that can serve as potential indicators for granite-pegmatite Nb–Ta deposits. Quartz in topaz–albite granite typically showcases Ti content exceeding 10 ppm and Ge/Ti ratios below 0.1, while pegmatites exhibit Ti content below 10 ppm and Ge/Ti ratios exceeding 0.1 (Fig. 9c). This finding aligns with previous work, suggesting that Ti < 10 ppm and Ge/Ti > 0.1 can be crucial indicators of highly evolved magmas and enriched rare metal elements. Most LCT-type pegmatites and some NYF-type pegmatites adhere to this criterion, while S-type granites deviate significantly. Interestingly, the pegmatites in Songshugang conform to this pattern, while the topaz–albite granite does not. This suggests that the Ti-Ge/Ti correlation in quartz is a key indicator for granite-pegmatite Nb–Ta mineralization in the Songshugang area and potentially beyond.

LA–ICP–MS analysis delves deeper into the magmatic-hydrothermal system, revealing significantly higher K and Na content in the quartz from topaz–albite granite compared to other rock types, while the Ca content in the quartz from quartz–fluorite pegmatite decreases, coinciding with the presence of fluorite minerals. These findings suggest a magma-hydrothermal system enriched in volatile components like F, enhancing the solubility of rare metals like Nb, Ta, W, Sn, and others. Additionally, the alteration zones in the Songshugang area, dominated by albitization, greisenization, and K-feldspathization, further support a similar magmatic evolution process. Moreover, increasing Al, Li, Ge, and Sb content in quartz trace elements, coupled with decreasing Ti content, can serve as additional markers for locating granite-pegmatite Nb–Ta deposits as magmatic evolution progresses.

By deciphering the tale whispered within the quartz of the Songshugang deposit, this study sheds light on its unique evolutionary path and identifies crucial geochemical signatures for exploration. The contrasting characteristics between topaz–albite granite and pegmatites, coupled with the Ti–Ge/Ti correlation in quartz and volatile signatures, provide valuable tools for locating similar Nb–Ta deposits, paving the way for efficient resource exploration not only in Songshugang but potentially in other regions with similar geological settings.

6 Conclusion

(1) The quartz from topaz–albite granite, quartz–mica pegmatite, and quartz–feldspar pegmatite, exhibits numerous dark CL streaks and patches, and a series of healed fractures under CL. These textures are closely linked to deep crustal pressure and hydrothermal fluid metasomatism. The quartz from quartz–fluorite pegmatite exhibits a distinct growth zone and the contents of Al, Li, Ge, and Sb vary widely, reflecting the melt-fluid composition imbalance at this stage.

(2) From topaz–albite granite, quartz–mica pegmatite, quartz–feldspar pegmatite, to quartz–fluorite pegmatite, Al, Li, Ge and Sb contents and Al/Ti, Ge /Ti, Sb/Ti ratios in quartz gradually increased, but Ti content gradually decreased, can effectively reflect the magmatic evolution trend; the enrichment of Na and K in topaz–albite granite and the reduction of Ca content in quartz–fluorite pegmatite indicate the occurrence of hydrothermal fluid metasomatism.

(3) Based on the characteristics of quartz CL texture (dark CL streaks and patches, and a series of healed fractures), trace elements (Al, Li, Ge, Sb, K, Na, Al/Ti, Ge /Ti, and Sb/Ti), and petrology, the Songshugang Nb–Ta mineralization is considered to be the result of magmatism and hydrothermal fluid metasomatism.

(4) Ti < 10 ppm and Ge/Ti > 0.1, as well as Al, Li, Ge, Sb contents and Al/Ti, Ge/Ti, Sb/Ti ratios in quartz are effective indicators of highly evolved magmas and rare metal element enrichment.

Authors' contributions Hengsong Zhang: Investigation, methodology, data curation, visualization, writing-original draft, and writing-review and editing; Shaohao Zou: Conceptualization, investigation, methodology, writing-original draft, writing-review and editing, supervision, funding acquisition; Xilian Chen: Investigation, writing-original draft, project administration; Deru Xu and Zhilin Wang: Writing-review and editing; Yongwen Zhang and Hua Wang: Sampling, writing-review, and editing.

Declarations

References

Akoh JU, Ogunleye PO, Ibrahim AA (2015) Geochemical evolution of micas and Sn-, Nb-, Ta- mineralization associated with the rare metal pegmatite in Angwan Doka, central Nigeria. J Afr Earth Sc 112:24–36

Ballouard C, Elburg MA, Tappe S, Reinke C, Ueckermann H, Doggart S (2020) Magmatic-hydrothermal evolution of rare metal pegmatites from the Mesoproterozoic Orange River pegmatite belt (Namaqualand, South Africa). Ore Geol Rev 116:103252

Bernet M, Bassett K (2005) Provenance analysis by single-quartz-grain SEM-CL/optical microscopy. J Sediment Res 75:492–500

Beurlen H, Müller A, Silva D, Da Silva MRR (2011) Petrogenetic significance of LA–ICP-MS trace-element data on quartz from the Borborema Pegmatite Province, northeast Brazil. Min Mag 75:2703–2719

Breiter K, Müller A (2009) Evolution of rare-metal granitic magmas documented by quartz chemistry. Eur J Min 21:335–346

Breiter K, Müller A, Leichmann J, Gabašová A (2005) Textural and chemical evolution of a fractionated granitic system: the Podlesí stock, Czech Republic. Lithos 80:323–345

Breiter K, Ackerman L, Ďurišová J, Svojtka M, Novák M (2014) Trace element composition of quartz from different types of pegmatites: a case study from the Moldanubian Zone of the Bohemian Massif (Czech Republic). Min Mag 78:703–722

Breiter K, Ďurišová J, Dosbaba M (2020) Chemical signature of quartz from S- and A-type rare-metal granites: A summary. Ore Geol Rev 125:103674

Che XD, Wang RC, Wu FY, Zhang WL, Hu H, Xie L, Lu JJ, Zhang D (2019) Episodic Nb–Ta mineralisation in South China: Constraints from in situ LA–ICP–MS columbite–tantalite U-Pb dating. Ore Geol Rev 105:71–85

Czamanske GK, Roedder E, Burns FC (1963) Neutron activation analysis of fluid inclusions for copper, manganese, and zinc. Science 140:401–403

Deng P, Chen YM, Jinhua JH, Zhang WB (2019) Study on the resource distribution and industry development of global niobium and tantalum. China Mining Mag 28:63–68 (**in Chinese with English abstract**)

Goodenough KM, Wall F, Merriman D (2018) The rare earth elements: Demand, global resources, and challenges for resourcing future generations. Nat Resour Res 27:201–216

Götze J (2009) Chemistry, textures and physical properties of quartz: Geological interpretation and technical application. Min Mag 73:645–671

Götze J, Plötze M, Habermann D (2001) Origin, spectral characteristics and practical applications of the cathodoluminescence (CL) of quartz: A review. Min Petrol 71:225–250

Götze J, Plötze M, Graupner T, Hallbauer DK, Bray CJ (2004) Trace element incorporation into quartz: A combined study by ICP–MS, electron spin resonance, cathodoluminescence, capillary ion analysis, and gas chromatography. Geochim Cosmochim Acta 68:3741–3759

He H, He M, Li JW (2018) Analysis of the niobium resources supply and demand pattern in China. China Min Mag 27:1–5 (**in Chinese with English abstract**)

Hong T, Hollings P, Gao J, Xu XW, Wu Q, Wu C, Mao Q (2020) Mineralization and petrogenesis of the Qiongheba porphyry copper deposit in Mengxi district, East Junggar, China. Ore Geol Rev 127:103848

Hua RM, Chen P, Zhang WL, Lu JJ (2005) Three large-scale metallogenic events related to the Yanshanian period in Southern China. In: Mao J, Bierlein FP (eds) Mineral deposit research: meeting the global challenge. Springer, Berlin Heidelberg, pp 401–404

Huang DT (1999) Origin of the Songshugang W–Sn–Nb–Ta polymetallic deposit, Jiangxi. Geol Explor Non-Ferr Metals 8:40–45 (**in Chinese with English abstract**)

Huang DT (2003) Evolving characteristics and related rare-metal metallogenesis off Lingshan rock body. Geol Prospect 39:35–40 (**in Chinese with English abstract**)

Jacamon F, Larsen RB (2009) Trace element evolution of quartz in the charnockitic Kleivan granite, SW-Norway: The Ge/Ti ratio of quartz as an index of igneous differentiation. Lithos 107:281–291

Jarchovský T (2006) The nature and genesis of greisen stocks at Krásno, Slavkovský les area: Western Bohemia, Czech Republic. J Geosci 51:201–216

Jiang XQ (2020) Geochemical characteristics and petrogenesis analysis of the metallogenic pluton of the Huangshan Nb–Ta deposit in Jiangxi. Dissertation, Chengdu University of Technology (**in Chinese with English abstract**)

Kanaori Y (1986) A SEM cathodoluminescence study of quartz in mildly deformed granite from the region of the Atotsugawa fault, central Japan. Tectonophysics 131:133–146

Landtwing MR, Pettke T (2005) Relationships between SEM-cathodoluminescence response and trace-element composition of hydrothermal vein quartz. Am Miner 90:122–131

Larsen RB, Henderson I, Ihlen PM, Jacamon F (2004) Distribution and petrogenetic behaviour of trace elements in granitic pegmatite quartz from South Norway. Contrib Min Petrol 147:615–628

Larsen RB, Jacamon F, Kronz A (2009) Trace element chemistry and textures of quartz during the magmatic hydrothermal transition of Oslo Rift granites. Min Mag 73:691–707

Leeman WP, MacRae CM, Wilson NC, Torpy A, Lee CTA, Student JJ, Thomas JB, Vicenzi EO (2012) A study of cathodoluminescence and trace element compositional zoning in natural quartz from volcanic rocks: Mapping titanium content in quartz. Microsc Microanal 18:1322–1341

Lehmann K, Pettke T, Ramseyer K (2011) Significance of trace elements in syntaxial quartz cement, Haushi Group sandstones, sultanate of Oman. Chem Geol 280:47–57

Li J, Huang XL, He PL, Li WX, Yu Y, Chen LL (2015) In-situ analyses of micas in the Yashan granite, South China: Constraints on magmatic and hydrothermal evolutions of W and Ta–Nb bearing granites. Ore Geol Rev 65:793–810

Li XF, Wei XL, Zhu YT, Li ZF, Deng XC (2021) Rare metal deposits in South China: Types, characteristics, distribution and tectonic setting. Acta Petrol Sin 37:3591–3614 (**in Chinese with English abstract**)

Linnen RL (1998) The solubility of Nb–Ta–Zr–Hf–W in granitic melts with Li and Li + F; constraints for mineralization in rare metal granites and pegmatites. Econ Geol 93:1013–1025

Linnen RL, Keppler H (1997) Columbite solubility in granitic melts: consequences for the enrichment and fractionation of Nb and Ta in the Earth's Crust. Contrib Miner Petrol 128:213–227

Linnen RL, Samson IM, Williams-Jones AE, Chakhmouradian AR (2014) Geochemistry of the rare-earth element, Nb, Ta, Hf, and Zr deposits. In: Treatise on geochemistry. Elsevier, pp 543–568

Liu T (2023) Magmatic-hydrothermal evolution and Nb–Ta mineralization in the Lingshan complex, Southeast China. Dissertation, China University of Geosciences (**in Chinese with English abstract**)

Mao JW, Xie GQ, Li XF, Zhang CQ, Wang YT (2010) Mesozoic Large-scale mineralization and multiple lithospheric extensions in South China. Acta Geol Sin: Engl Ed 80:420–431

Melcher F, Graupner T, Gäbler H-E et al (2015) Tantalum–(niobium–tin) mineralisation in African pegmatites and rare metal granites: constraints from Ta–Nb oxide mineralogy, geochemistry and U-Pb geochronology. Ore Geol Rev 64:667–719

Monecke T, Kempe U, Götze J (2002) Genetic significance of the trace element content in metamorphic and hydrothermal quartz: a reconnaissance study. Earth Planet Sci Lett 202:709–724

Müller A, Koch-Müller M (2009) Hydrogen speciation and trace element contents of igneous, hydrothermal and metamorphic quartz from Norway. Mineral Mag 73:569–583

Müller A, Seltmann R, Behr H (2000) Application of cathodoluminescence to magmatic quartz in a tin granite–case study from the Schellerhau Granite Complex, Eastern Erzgebirge. Ger Miner Depos 35:169–189

Müller A, Wiedenbeck M, Van Den Kerkhof AM, Kronz A, Simon K (2003) Trace elements in quartz: a combined electron microprobe, secondary ion mass spectrometry, laser-ablation ICP–MS, and cathodoluminescence study. Eur J Mineral 15:747–763

Müller A, Breiter K, Seltmann R, Pécsay Z (2005) Quartz and feldspar zoning in the eastern Erzgebirge volcano-plutonic complex (Germany, Czech Republic): Evidence of multiple magma mixing. Lithos 80:201–227

Müller A, Ihlen PM, Kronz A (2008) Quartz chemistry in polygeneration Sveconorwegian pegmatites, Froland, Norway. Eur J Mineral 20:447–463

Müller A, Herrington R, Armstrong R, Seltmann R, Kirwin DJ, Stenina NG, Kronz A (2010) Trace elements and cathodoluminescence of quartz in stockwork veins of Mongolian porphyry-style deposits. Miner Deposita 45:707–727

Müller A, Wanvik JE, Ihlen PM (2012) Petrological and chemical characterisation of high-purity quartz deposits with examples from Norway. In: Götze J, Möckel R (eds) Quartz: Deposits, mineralogy and analytics. Springer, Berlin Heidelberg, pp 71–118

Müller A, Keyser W, Simmons WB, Webber K, Wise M, Beurlen H, Garate-Olave I, Roda-Robles E, Galliski MÁ (2021) Quartz chemistry of granitic pegmatites: Implications for classification, genesis and exploration. Chem Geol 584:120507

Nardi LVS, Formoso MLL, Jarvis K, Oliveira L, Bastos Neto AC, Fontana E (2012) REE, Y, Nb, U, and Th contents and tetrad effect in zircon from a magmatic-hydrothermal F-rich system of Sn-rare metal–cryolite mineralized granites from the Pitinga Mine, Amazonia, Brazil. J S Am Earth Sci 33:34–42

Paton C, Hellstrom J, Paul B, Woodhead J, Hergt J (2011) Iolite: Freeware for the visualisation and processing of mass spectrometric data. J Anal Spectrom 26:2508–2518

Rottier B, Casanova V (2021) Trace element composition of quartz from porphyry systems: A tracer of the mineralizing fluid evolution. Miner Depos 56:843–862

Ruffini R, Borghi A, Cossio R, Olmi F, Vaggelli G (2002) Volcanic quartz growth zoning identified by cathodoluminescence and EPMA studies. Microchim Acta 139:151–158

Rusk B (2012) Cathodoluminescent textures and trace elements in hydrothermal quartz. In: Götze J, Möckel R (eds) Quartz: Deposits, mineralogy and analytics. Springer, Berlin Heidelberg, pp 307–329

Rusk BG, Reed MH, Dilles JH, Kent JR (2006) Intensity of quartz cathodoluminescence and trace-element content in quartz from the porphyry copper deposit at Butte. Mont Am Mineral 91:1300–1312

Rusk BG, Lowers HA, Reed MH (2008) Trace elements in hydrothermal quartz: Relationships to cathodoluminescent textures and insights into vein formation. Geology 36:547

Schieber J, Krinsley D, Tennison E (2002) Provenance studies of fine-grained sediments with scanned cathodoluminescence of quartz: Potential applications in planetary exploration. Lunar and Planetary Science. p 1088

Schrön W, Schmädicke E, Thomas R, Schmidt W (1988) Geochemische Untersuchungen an Pegmatitquarzen. Z Geol Wiss 16:229–244 (**in German**)

Seyedolali A, Krinsley DH, Boggs S, O'Hara PF, Dypvik H, Goles GG (1997) Provenance interpretation of quartz by scanning electron microscope–cathodoluminescence fabric analysis. Geology 25:787

Siegel K, Vasyukova OV, Williams-Jones AE (2018) Magmatic evolution and controls on rare metal-enrichment of the Strange Lake A-type peralkaline granitic pluton. Québec-Labrador Lithos 308–309:34–52

Stevens-Kalceff MA (2009) Cathodoluminescence microcharacterization of point defects in α-quartz. Mineral Mag 73:585–605

Sun T (2006) A new map showing the distribution of granites in South China and its explanatory notes. Geol Bull China 25:332–335 (**in Chinese with English abstract**)

Thomas R, Förster H-J, Rickers K, Webster JD (2005) Formation of extremely F-rich hydrous melt fractions and hydrothermal fluids during differentiation of highly evolved tin-granite magmas: A melt/fluid-inclusion study. Contrib Mineral Petrol 148:582–601

Thomas JB, Bruce Watson E, Spear FS, Shemella PT, Nayak SK, Lanzirotti A (2010) TitaniQ under pressure: The effect of pressure and temperature on the solubility of Ti in quartz. Contrib Mineral Petrol 160:743–759

Van Den Kerkhof AM, Kronz A, Simon K, Riganti A, Scherer T (2004) Origin and evolution of Archean quartzites from the Nondweni greenstone belt (South Africa): Inferences from a multidisciplinary study. S Afr J Geol 107:559–576

Van Lichtervelde M, Holtz F, Melcher F (2018) The effect of disequilibrium crystallization on Nb–Ta fractionation in pegmatites: Constraints from crystallization experiments of tantalite-tapiolite. Am Miner 103:1401–1416

Wang DZ, Zhou JC (2005) New progress in studying the large igneous provinces. Geol J China Univ 11:1–8 (**in Chinese with English abstract**)

Wang YR, Li JT, Lu JL, Fan WL (1982) Geochemical mechanism of Nb-, Ta-mineralization during the late stage of granite crystallization. Geochemistry 1:175–185

Wang FL, Zhao TP, Chen W (2012) Advances in study of Nb–Ta ore deposits in Panxi area and tentative discussion on genesis of these ore deposits. Mineral Depos 31:293–308 (**in Chinese with English abstract**)

Wang XN, Chen XL, Zou SH, Jia ZW, Li B, Wang H, Xu DR (2023) Geochronology, geochemistry, and mineral chemistry of the Lingshan-Huangshan complex, South China: Insights into Nb and Ta enrichment. Ore Geol Rev 157:105433

Wark DA, Watson EB (2006) TitaniQ: A titanium-in-quartz geothermometer. Contrib Mineral Petrol 152:743–754

Watt GR, Wright P, Galloway S, McLean C (1997) Cathodoluminescence and trace element zoning in quartz phenocrysts and xenocrysts. Geochim Cosmochim Acta 61:4337–4348

Wu MQ, Samson IM, Zhang DH (2018) Textural features and chemical evolution in Ta–Nb oxides: Implications for deuteric Rare-metal mineralization in the Yichun Granite-marginal pegmatite, Southeastern China. Econ Geol 113:937–960

Xiang YX, Yang JH, Chen JY, Zhang Y (2017) Petrogenesis of Lingshan highly fractionated granites in the Southeast China: Implication for Nb–Ta mineralization. Ore Geol Rev 89:495–525

Xie L, Wang RC, Groat LA, Zhu JC, Huang FF, Cempírek J (2015) A combined EMPA and LA–ICP–MS study of Li-bearing mica and Sn–Ti oxide minerals from the Qiguling topaz rhyolite (Qitianling District, China): The role of fluorine in origin of tin mineralization. Ore Geol Rev 65:779–792

Xie L, Wang RC, Che XD, Huang FF, Erdmann S, Zhang WL (2016) Tracking magmatic and hydrothermal Nb–Ta–W–Sn fractionation using mineral textures and composition: A case study from the Late Cretaceous Jiepailing ore district in the Nanling Range in South China. Ore Geol Rev 78:300–321

Zajacz Z, Halter WE, Pettke T, Guillong M (2008) Determination of fluid/melt partition coefficients by LA-ICPMS analysis of co-existing fluid and silicate melt inclusions: Controls on element partitioning. Geochim Cosmochim Acta 72:2169–2197

Zaraisky GP, Korzhinskaya V, Kotova N (2010) Experimental studies of Ta_2O_5 and columbite–tantalite solubility in fluoride solutions from 300 to 550°C and 50 to 100 MPa. Miner Petrol 99:287–300

Zhao ZH, Chen HY, Han JS (2022) Rare metal mineralization of the Mesozoic pegmatite in Altay orogeny, northern Xinjiang. Acta Sci Natur Univ Sunyatseni 61:1–26 (**in Chinese with English abstract**)

Zhong JS, Ji X (2017) Geological characteristics and enrichment law of Tantalum–Niobium deposit in Songshugang of Geyuan country. World Nonferrous Metals 15:181–182 (**in Chinese with English abstract**)

Zhou XM, Sun T, Shen W, Shu L, Niu Y (2006) Petrogenesis of Mesozoic granitoids and volcanic rocks in south China: A response to tectonic evolution. Episodes 29:26–33

Zhu ZY, Wang RC, Che XD, Zhu JC, Wei XL, Huang XE (2015) Magmatic–hydrothermal rare-element mineralization in the Songshugang granite (northeastern Jiangxi, China): Insights from an electron-microprobe study of Nb–Ta–Zr minerals. Ore Geol Rev 65:749–760

Zhu ZY, Wang RC, Marignac C, Cuney M, Mercadier J, Che XD, Lespinasse MY (2018) A new style of rare metal granite with Nb-rich mica: The early cretaceous Huangshan rare-metal granite suite, northeast Jiangxi Province, southeast China. Am Miner 103:1530–1544

Zhu ZY, Wang RC, Marignac C, Cuney M, Mercadier J, Che XD, Charles N, Lespinasse M (2019) Petrogenesis of Nb–(Ta) aplo-pegmatites and fine-grained granites from the Early Cretaceous Huangshan rare-metal granite suite, northeast Jiangxi Province, southeast China. Lithos 346–347:105150